CrossMark

Cryogenic gamma detectors enable direct detection of ^{236}U and minor actinides for non-destructive assay

Miguel Velazquez[1,3] · Jonathan Dreyer[1] · Owen B. Drury[1] · Saleem Salaymeh[2] ·
Stephan Friedrich[1]

Abstract We demonstrate the utility of a superconducting transition edge sensor (TES) γ-ray detector with high energy resolution and low Compton background for non-destructive assay (NDA) of a uranium sample from reprocessed nuclear fuel. We show that TES γ-detectors can separate low-energy actinide γ-emissions from the background and nearby lines, even from minor isotopes whose signals are often obscured in NDA with conventional Ge detectors. Superconducting γ-detectors may therefore bridge the gap between high-accuracy destructive assay (DA) and easier-to-use NDA.

Introduction

Non-destructive assay (NDA) with high-resolution γ-detectors is widely used to measure the isotopic composition of nuclear materials [1]. Although NDA is not as accurate as destructive analysis (DA) by mass spectrometry (MS), it is simpler, faster, and therefore more cost effective and preferred for initial sample screening or when moderate accuracy is sufficient. NDA with γ-detectors infers isotope ratios in nuclear materials from the measured intensity ratio of γ-emissions from different isotopes. For highest accuracy, NDA is based on γ-emissions with similar energies to reduce systematic errors due to variations in detection efficiency. This can lead to line overlap and errors due to the finite energy resolution of the high-purity germanium (HPGe) detectors that are typically used [1, 2]. In addition, although the lines with highest branching ratios often occur at very low energies, HPGe detectors have a high Compton background in that region that can obscure γ-emissions from minor isotopes.

Cryogenic γ-ray detectors with operating temperatures of ∼100 mK offer an energy resolution ∼10 × higher than HPGe γ-detectors and can therefore address the line-overlap problems in NDA [3–7]. The detector volumes also tend to be small, which is generally disadvantageous due to the reduction in detection efficiency, but does reduce the Compton background for NDA at very low energies. Cryogenic detectors have been developed for the last three decades and are increasingly used for a variety of scientific applications [8]. Here we demonstrate the use of cryogenic γ-detectors for non-destructive assay of a mixed isotope uranium sample from reprocessed nuclear fuel.

Experimental

Sample preparation

A highly enriched uranium sample that was being analyzed at SRNL was chosen for high-resolution low energy γ-ray/X-ray analysis. It came originally from the Y-12 facility and contained uranium "skull oxide", a term that refers to metal fragments from a uranium casting process that have been

✉ Stephan Friedrich
friedrich1@llnl.gov

1 Lawrence Livermore National Laboratory, 7000 East Ave, Livermore, CA 94550, USA

2 Savannah River National Laboratory, Building 737-A, Aiken, SC 29802, USA

3 Present Address: INAOE, Santa Maria Tonatzintla 72840, Puebla, Mexico

Springer

oxidized in a furnace. The isotopic abundance for the materials characterized at Y-12 was nominally 91 atomic % ^{235}U with 2 atomic % ^{233}U, and the remainder mostly ^{238}U and some minor actinides. As a reference, the uranium isotopic composition was determined more accurately at SRNL by inductively-coupled plasma mass spectrometry (ICP-MS) (Table 1, column 2). The component of the ICM-MS analysis with mass 232 was attributed to ^{232}U. The ICP-MS values of the uranium concentrations agreed with the Y-12 declarations within the analytical uncertainly.

For NDA at SRNL, 0.05 ml aliquots of the sample solution were pipetted onto small platinum planchets and evaporated to dryness under a heat lamp. The planchets were heated cherry red in the flame of a propane Bunsen burner to fuse the activity into them. The samples were then analyzed at the SRNL counting facilities, first with a 20 mm thick, 2000 mm^2 area semi-planar low-energy Ge detector (LE Ge) with carbon composite windows to observe the low energy γ-ray/X-ray spectra. They were subsequently assayed using a nominally 40 % efficient coaxial HPGe (Coax Ge) detector and a Si alpha spectrometer. The activity of different isotopes in the sample as measured by alpha spectrometry is shown in Table 1 (column 4).

For the experiments with superconducting γ-detectors at LLNL, 0.05 ml aliquots of the skull oxide solution were dried inside an Al holder designed for mounting close to the detector at low temperatures. A small amount of epoxy was spread over the back of the sample to affix the material to the holder and seal it inside, and an Al cover was screwed on for secondary containment.

Superconducting gamma detector

The cryogenic γ-detector for this experiment was based on a superconducting Mo/Cu transition edge sensor (TES) with a 1 mm × 1 mm × 0.25 mm Sn absorber [3, 6, 9]. The detector and the skull oxide sample were held at the end of a cold finger of an adiabatic demagnetization refrigerator (ADR) whose temperature was regulated at 90

Table 1 DA and NDA isotope analysis of the skull oxide sample. The error on the ICP-MS measurements was 2 %. The ICP-MS signal with mass 232 was tentatively attributed to uranium

Isotope (DA)	ICP-MS (%)	Isotope (NDA)	NDA (dpm ± 1σ)
^{232}U (?)	0.07 %	^{208}Tl	6.3 ×10^3 ± 10 %
^{233}U	1.59 %	^{212}Bi	2.1 ×10^4 ± 10 %
^{234}U	0.83 %	^{212}Pb	2.0 ×10^4 ± 10 %
^{235}U	89.99 %	^{224}Ra	2.0 ×10^4 ± 10 %
^{236}U	0.43 %	^{235}U	2.4 ×10^4 ± 10 %
^{238}U	7.08 %	^{238}Pu	9.3 ×10^5 ± 10 %
		^{241}Am	1.9 ×10^3 ± 30 %
		$^{239/240}$Pu	1.6 ×10^4 ± 20 %

mK. Gamma-induced pulses were read out with a SQUID pre-amplifier and optimally filtered off-line. Since the total activity of the sample was low and the active area of the superconducting detector pixel was only ∼1 mm^2, the data acquisition rate was only 0.5 counts/s. In addition, the ADR hold time at 90 mK was only ∼6 h per magnetization cycle, and several 6-h spectra were therefore taken to improve statistics. The spectra were calibrated independently and added. For short intervals, the detector resolution varied between ∼90 and ∼150 eV FWHM. However, detector non-linearities and drift in the detector response over time, most likely due to different degrees of flux trapping in the superconducting sensor, degraded the resolution of the combined spectrum to ∼250 eV FWHM and caused a non-Gaussian component in the line shape. This energy resolution was still sufficient to identify γ-emissions from minor isotopes in the sample.

Results and discussion

The analysis focuses on the low-energy region of the spectrum where cryogenic detectors are most useful because γ-emissions are strong and often closely spaced, and the detectors' high resolution and low Compton background favor the identification of lines from minor isotopes. Figure 1 shows the spectral region from 5 to 25 keV that is dominated by L-shell X-rays. Spectra from the two Ge detectors are included for comparison. As expected, they show X-rays from the daughter products (U, Pa, Th, Ra) and from materials surrounding the source (Pt) and the detector (Cu, Au, Pb, In). This spectral region is typically ignored for NDA, because Ge detectors can often not resolve the individual lines, although it does contain some of the strongest actinide emissions. For example,
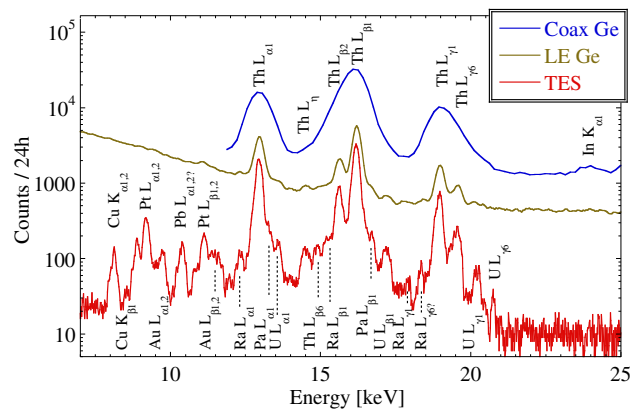
Fig. 1 The spectrum of the uranium skull oxide sample below 25 keV, as measured with a superconducting TES and two HPGe γ-detectors. It is dominated by the L-shell X-rays of the daughter products from the sample and secondary excitation of materials surrounding the detector

given that the source is weak and secondary excitation of uranium is negligible, the observation of uranium X-rays suggests the presence of Pu and indicates the source of the material from reprocessed fuel.

The region between 25 and 70 keV contains some of the actinide γ-rays with the highest branching ratios, but again, this region is not widely used for NDA. Figure 2 illustrates that superconducting TES detectors can resolve many of the characteristic γ-rays above the spectral background, despite the significantly lower number of total counts for a single TES detector during the same 24-h acquisition time. Even a small Ge detector whose energy resolution is limited by Fano statistics can only detect lines from the fissile uranium isotopes [233]U and (at higher energy) [235]U, while the [238]Pu and [239]Pu lines are too weak to rise above the Compton background. The superconducting detector, on the other hand, shows the two strongest [239]Pu γ-peaks at 51.624 and 38.661 keV, because its high energy resolution increases the peak amplitude and because its small pixel size reduces the Compton background by more than a factor of 25. Since no [240]Pu signal is observed at 45.242 keV, although this line has a branching ratio of 0.045 % (compared to 0.027 % for the strongest [239]Pu line at 51.624 keV), the NDA alpha signal for this sample must be predominantly due to [239]Pu (cf. Table 1). Similarly, the TES spectrum clearly shows the strongest U-233 γ-rays at 42.44, 54.699 and 29.192 keV, but no [232]U signal at 57.766 keV. This is despite the fact that the shorter [232]U half life of 69 years (compared to 159,200 years for [233]U) and the 0.2 % branching ratio of the [232]U line at 57.766 keV (compared to 0.0862 % for the [233]U line at 42.44 keV) more than compensate for the low measured [232]U concentration of 0.07 % (compared to 1.59 % [233]U). This suggests that the component of the ICM-MS analysis with mass 232 is due to a different element. The spectrum also shows a weak line at 28 keV that we have not yet been able to assign to the emission from any isotope. Neither can we explain it as an escape line from the Sn absorber, because many strong peaks in the spectrum do not cause similar lines from the escape of Sn K X-ray with energies of 25.044, 25.271, and 28.486 keV.

Finally, the TES γ-spectrum shows evidence of [236]U. This isotope is interesting because it does not occur naturally, and its presence indicates that the uranium sample has been exposed to neutrons that have been captured on [235]U. [236]U is difficult to detect by γ-spectroscopy, because its two γ-rays at 49.369 at 112.75 keV are weak and very close to the 49.55 and 113.5 keV lines from [238]U, an isotope that is typically present in much higher concentration. Our cryogenic γ-detectors observe a peak ∼49.5 keV, close to the expected energy for [236]U, but still ∼130 eV from the literature value and closer to the energy of [238]U. But the ICP-MS analysis of the uranium isotopes (Table 1) and the literature values of the half lives and branching ratios [10] predict a [236]U line > 10 × stronger than the [238]U line, primarily due to the ∼200 × shorter half life of [236]U. Interestingly, the branching ratio of the [236]U γ-ray at 49.369 keV appears to have only been calculated [10] or measured relative to the strength of the other lines in the decay of [236]U [11]. This could imply either that the branching ratio for the [236]U γ-ray is much lower than its literature value, or that the peak in the spectrum is shifted from its expected position.

Figure 2 shows both the strength and the limitation of our superconducting TES γ-detectors. One problem is that the TES response is non-linear and can change slightly over time and between cool-downs. This non-linearity can require an energy calibration based on higher-order polynomials or cubic spline fits, as observed by other groups [7], with details depending on the specific detector fabrication and the experimental setup. While such an energy resolution ensures that strong calibration lines are assigned the correct energy, the weaker lines between the calibration points can be shifted if the detector is non-linear, or broadened if its response changes between runs. These effects also produce non-Gaussian line shapes, and can wash out weak lines to the point that they are no longer detectable above the Compton background.

In addition, published reference data for γ-energies can vary by several tens of eV. This can make it difficult to distinguish between detector non-linearities and systematic calibration errors. Cryogenic gamma detectors can help reduce these errors and thus set the stage for NDA at very low energies.

Conclusions

We have illustrated the utility of superconducting γ-detectors for isotope analysis at energies below 100 keV. Although this spectral region is rich in information because
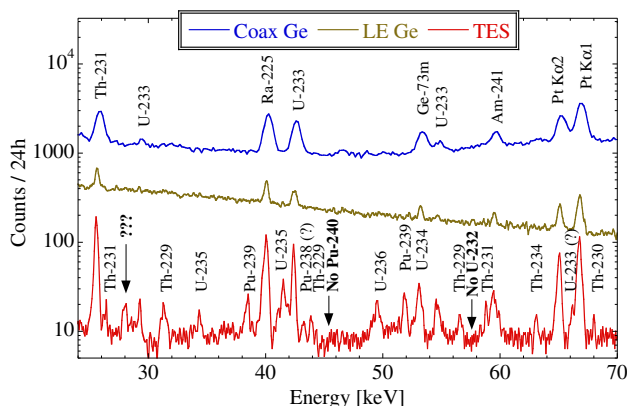
Fig. 2 The low-energy TES γ-spectrum of the skull oxide shows many actinide lines not detected with HPGe detectors. The TES data have been smoothed to reduce statistical noise

of the multitude of lines, it is not often used for NDA with HPGe γ-detectors, which can have a high Compton background and insufficient energy resolution to identify and separate individual lines. Superconducting TES γ-detectors allow NDA of nuclear materials at energies below 100 keV where many actinides produce high intensity γ-lines. Their high energy resolution and low Compton background enables the detection of γ-emissions that are obscured in HPGe spectra. This can increase the sensitivity for NDA of weakly radioactive samples. On the other hand, it will be necessary to improve the stability and linearity of our TES detector response for consistent line shapes during long acquisitions. In addition, higher accuracy measurements of γ-energies and branching ratios will be required to reduce systematic NDA errors. Cryogenic detectors can contribute to this goal, but their linearity and detection efficiency need to be improved to fully exploit their potential benefits, especially at very low energy.

References

1. Reilly D, Ensslin N, Smith H, Kreiner S (1991), Passive non-destructive assay of nuclear materials, NUREG/CR-5550, Washington
2. Zhao K et al (2010), International Target Values 2010 for Measurement Uncertainties in Safeguarding Nuclear Materials, IAEA STR-368, Vienna
3. Cunningham F et al (2002) High-resolution operation of frequency-multiplexed transition-edge photon sensors. Appl Phys Lett 81:159–161
4. Fleischmann A, Enss C, Seidel G (2005) Metallic magnetic calorimeters. Top Appl Phys 99:151–216
5. Zink BL et al (2006) Array-compatible transition edge sensors microcalorimeter γ-ray detector with 42 eV energy resolution at 103 keV. Appl Phys Lett 89:124101
6. Friedrich S (2007) Nuclear diagnostics with cryogenic detectors. Nucl Inst Meth A 579:157–160
7. Bennett DA, Horansky RD, Schmidt DR et al (2012) A high resolution γ-ray spectrometer based on superconducting microcalorimeters. Rev Sci Inst 83:093113
8. Enss C (ed) (2005) Cryogenic particle detection. Topics in Applied Physics, vol 99. Springer, Berlin
9. Drury OB, Velazquez M, Dreyer JG, Friedrich S (2009) Development of ultrahigh energy resolution gamma spectrometers for nuclear safeguards. J Radioanal Nucl Chem 282:913–917
10. WWW Table of Radioactive Isotopes, http://ie.lbl.gov/toi/
11. Gehrke RJ, Baker JD, Riddle CL (2002) Feeding of the ^{232}Th levels from the decay of ^{236}U. Appl Rad Isotopes 56:567–568